

The role of T-helper/T-regulator lymphocyte ratio on the adaptive immune response: a mathematical model

Alessia Annibale

Department of Mathematics, King's College London, The Strand, London WC2R 2LS, UK
 Institute for Mathematical and Molecular Biomedicine, King's College London, Hodgkin Building, London SE1 1UL, UK

Abstract

In this work we use a combination of statistical physics and dynamical systems approaches, to analyze the response to an antigen of a simplified model of the adaptive immune system, which comprises B, T helper and T regulatory lymphocytes. Results show that the model is remarkably robust against changes in the kinetic parameters, noise levels, and mechanisms that activate T regulatory lymphocytes. In contrast, the model is extremely sensitive to changes in the ratio between T helper and T regulatory lymphocytes, exhibiting in particular a phase transition, from a responsive to an immuno-suppressed phase, when the ratio is lowered below a critical value. To the best of our knowledge, this is the first mathematical study to support the validity of the T-helper/T-regulator lymphocyte ratio as an index of immunosuppression, with a potential for prognostic monitoring.

1 Introduction

Recent years have seen a surge of mathematical and computational models of the immune system, ranging from ordinary differential equations approaches [1, 2, 3, 4, 5, 6], agent-based models [7, 8, 9, 10] and stochastic dynamics [11, 12, 13, 14], to statistical mechanical models [15, 16, 17, 18, 19, 20], network approaches [21, 22] and machine learning [23, 24, 25, 26, 27]. For recent reviews, see [28, 29]. One of the reasons, is that the rapid improvement of data storage capacity and experimental techniques, has led to an explosion of data, meaning that quantitative tools are needed to interpret and efficiently extract in-

formation from them. Another reason is that, while experiments in vitro and in mice have provided tremendous insights into the immune systems, the extrapolation of results to humans is not always obvious [30], so theoretical frameworks are demanded to model the immune system in humans, where experimental work is very limited.

A major area of focus in immunology in recent years has been regulatory T cells, which suppress other immune cells. These are believed to have several important functions, including maintenance of homeostasis, immunological unresponsiveness to self-antigens, and prevention of autoimmune diseases [31], and in the last few years have witnessed an explosion of knowledge driven by detailed experimental work [32, 33, 34].

In addition, recent studies have suggested that the imbalance between regulatory and conventional T cells may be an index of immunosuppression in cancer patients [35, 36], and may play a crucial role in the progression of HIV infections and response to antiretroviral therapies [37, 38, 39], immunosenescence [40] and in inflammation and autoimmune diseases [41]. However, the lack of reliable markers for distinguishing regulatory from conventional T cells, and variations in the total lymphocyte count make regulatory T cells counting controversial [36] and a general consensus on the validity of the imbalance of regulatory T cells as a therapeutic target or tool for prognostic monitoring has not been achieved.

While many mathematical models have been developed to understand how regulatory T cells promote immunological tolerance towards self-antigens (see [42, 43] for a review), an understanding of the effect of the regulatory T cells imbalance on immunosuppression has lagged behind data ac-

quisition. In this work we propose a mathematical model of the adaptive immune system that is aimed at filling this gap. In Section 2 we summarize the key mechanisms that regulate the adaptive immune response. In Section 3 we set-up a minimal mathematical model for the adaptive immune system, comprising conventional and regulatory T cells and B cells and we study its response to an antigen, in a wide range of the parameters space and for different mechanisms for regulatory T cell activation. Finally in Section 4 we summarize our results and propose pathways for future work.

2 The adaptive immune system

The adaptive immune system is a complex network of cells that work together to defend the body against pathogens such as bacteria, virus or tumor cells. The most important types of cells that constitute it, are the lymphocytes, which can be divided into B and T cells.

B cells are equipped with B cell receptors (BCR), which are able to bind to specific pathogens. When a B cell comes across a pathogen that can bind its receptors, it ingests it, partially degrades it, and exports fragments of it, i.e. antigens, to the cell surface, where they are presented in association with proteins known as MHC molecules. Each B cell has a number $n = \mathcal{O}(10^4)$ of identical BCR on its surface.

T cells can be divided into T killers, that destroy infected or cancer cells, and T helpers, who have the role of signaling B cells and initiate an immune response. Similarly to B cells, T helper cells are equipped with receptors (TCR), but in contrast to B cells, they do not bind to the antigen directly, but to the MHC-antigen complex on the surface of antigen presenting cells (APC), such as B cells and other immune cells (e.g. dendritic cells). T helper cells have been commonly divided into T regulatory (Treg) cells and conventional T helper (Th) cells. When a Th cell binds an APC, it gets activated and starts proliferating while releasing proteins called cytokines, which activate B cells.

Once activated, B cells undergo clonal expansion, i.e. form many copies of identical cells sharing the same antigen receptors, and secrete antibodies, i.e. a free form of those receptors, that can recognize and neutralize the antigen. Clonal expansion usually involves migration of B cells to

the germinal centre¹, where B cells proliferate at a rate that is unparalleled in mammalian tissues. Random mutations during clonal expansion cause the production of antibodies with a broad range of binding affinities for their antigen. B cells with unfavourable mutations will not get sufficiently activated by the antigen and T cells, and will die, while those with improved affinity will be stimulated to clone themselves. This leads to an effective affinity-dependent selection process, within the germinal centre, known as affinity maturation [44], which results in an increase of affinity, by several orders of magnitude, over a time of one week in mammals.

Treg cells turn off antibody production and suppress the immune response. The mechanistic details of Treg cells functioning are still debated [45, 46]. For example, it is not clear whether their activation relies on antigens, in the same fashion as conventional Th cells, and whether Treg cells can directly suppress B cells or whether they must suppress Th cells in order to suppress B cells. Suppression of Th cells has been extensively modelled in the context of tolerance (see e.g. references in [42, 29]). In this work we model the direct suppression of B cells, which has been suggested in a number of recent studies (see e.g. [47, 48, 49, 50]).

2.1 The main reactions

As explained above, the activation of the adaptive immune system involves several reactions between lymphocytes and other immune cells, mediated or not by the antigen. Here we summarize the reactions that we shall include in our model:

- Antigens (Ag) replicate at a rate r

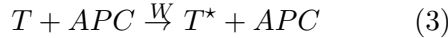


- B-cells bind to antigens via B cell receptors to form antigen presenting cells at a rate π^+ which depends on the affinity between the BCR and the antigen



¹Germinal centres are transient structures that form within peripheral lymphoid organs in response to T cell-dependent activation.

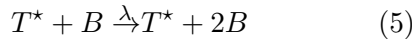
- T cells get activated when they bind an APC, at a rate W



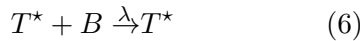
- APCs are eliminated at a rate π^- (e.g. by macrophages or via apoptosis)



- activated T cells stimulate B clonal expansion



or repress it



depending on the nature (Treg or Th) of the T cell

- B cells are kept in a state of activated apoptosis while undergoing clonal expansion in the germinal centre and compete for survival signal from T helper cells (germinal centre selection)



We will neglect, in our model, the presence of other immune cells that can serve as APC (e.g. dendritic cells) and we will neglect several other processes, such as antigen mutation, clonal expansion of T cells, activation (by T helper cells) of T killers, macrophages and other types of immune cells, production of antibodies by B cells, and affinity maturation of B cells in the germinal centre. We will simply assume that, due to this process, the affinity π^+ between BCR and antigen is an increasing function of time. Despite its simplicity, we believe that this model captures the basic principles of an immune response to an antigen and, to the best of our knowledge, it is the first quantitative model that reveals the ratio between Th and Treg cells as the single most important parameter that affects its behavior.

3 The mathematical set-up

We consider a population of T cells, each labelled by $i = 1, \dots, N$, and a population of B clones²,

²A B clone is the ensemble of all B cells that have the same receptors and thus respond to the same antigen.

each labelled by $\mu = 1, \dots, P$. We assume that each B clone μ is able to bind to one type of antigen (for simplicity assumed to have a single epitope) also labelled by μ . We denote by ψ_μ , b_μ and p_μ , the population densities of antigen type μ , B clone μ and B cells presenting antigen μ (i.e. APC of type μ), respectively. Experimental lymphocytes counts, estimate the total number of B cells to be αN with $\alpha \simeq 1/2$. We will assume that the number of B clones is sub-extensive in N , i.e. $P = \alpha N^\gamma$, with $\gamma \in (0, 1)$, so that each clone will contain on average a number $\mathcal{O}(N^{1-\gamma})$ of B cells.³ It is then convenient to define clonal densities as $b_\mu = B_\mu/cN^{1-\gamma}$ where B_μ is the size of B clone μ and $c = \mathcal{O}(N^0)$ is a constant that will be defined later, and similarly for $p_\mu = P_\mu/cN^{1-\gamma}$ and $\psi_\mu = \Psi_\mu/cN^{1-\gamma}$. We can then write the following equations, describing reactions (1), (2) and (4)

$$\frac{d}{dt}p_\mu = \pi_\mu^+ \psi_\mu b_\mu - \pi_\mu^- p_\mu \quad (8)$$

$$\frac{d}{dt}\psi_\mu = r_\mu \psi_\mu - \pi_\mu^+ \psi_\mu b_\mu \quad (9)$$

For each T cell i , we introduce a variable η_i which takes values 1 if i is helper and -1 if it is regulator. We assume each η_i to be identically and independently sampled from

$$P(\eta) = \frac{1+\epsilon}{2}\delta_{\eta,1} + \frac{1-\epsilon}{2}\delta_{\eta,-1} \quad (10)$$

The parameter $-1 \leq \epsilon \leq 1$ quantifies the imbalance between Th ($\eta = 1$) and Treg ($\eta = -1$) and is directly related to the T-helper/T-regulator lymphocyte ratio R , measured in experiments, via

$$R = \frac{1+\epsilon}{1-\epsilon}. \quad (11)$$

For $\epsilon = 0$ one has that Th and Treg are present in equal proportions, both equal to $1/2$ (i.e. $R = 1$), for $\epsilon > 0$ Th cells are more than Treg cells ($R > 1$) and for $\epsilon < 0$ Th cells are less than Treg cells ($R < 1$).

We represent the state of each T cell i (active or inactive) with a variable σ_i which takes value 1 if i is active and 0 otherwise. Helper T cells get activated via reaction (3), i.e. when their receptors

³The proposed scaling is consistent with experimental counts of lymphocytes, that estimate the number of T lymphocytes to be approximately $N = \mathcal{O}(10^{12})$, the number of B clones to be $P = \mathcal{O}(10^8)$, and the size of a clone at rest to be $\mathcal{O}(10^4)$.

bind to an APC. Assuming for simplicity that T cells update their state at regular time intervals of duration Δ , we have

$$\sigma_i(t + \Delta) = \theta\left(\sum_{\mu} \zeta_i^{\mu} p_{\mu}(t) - Tz(t)\right) \quad (12)$$

where $\theta(x)$ is the step function, taking values $\theta(x) = 0$ for $x \leq 0$ and $\theta(x) = 1$ for $x > 0$, z is a zero-averaged random variable with suitably normalised variance, drawn from some symmetric distribution $p(z)$, which mimicks biological noise, T is the noise strength, and $\zeta_i^{\mu} \in \{1, 0\}$ indicates whether (1) or not (0) T cell i can bind a cell in B clone μ . We assume the variables $\{\zeta_i^{\mu}\}$ to be identically and independently distributed according to

$$p(\zeta_i^{\mu}) = \frac{c}{N^{\gamma}} \delta_{\zeta_i^{\mu}, 1} + \left(1 - \frac{c}{N^{\gamma}}\right) \delta_{\zeta_i^{\mu}, 0} \quad (13)$$

so that each T cell i can signal an average number $\langle \sum_{\mu=1}^P \zeta_i^{\mu} \rangle = \alpha c$ of B clones and each B clone μ can be signaled, on average, by $\langle \sum_{i=1}^N \zeta_i^{\mu} \rangle = cN^{1-\gamma}$ T cells. Since the number of B cells in each clone is on average $\mathcal{O}(N^{1-\gamma})$, the choice (13) corresponds to the scenario where the number of T cells that can signal a B clone is of the same order as the number of B cells in that clone. Biologically, this would seem the most efficient and economical scenario, as it avoids, on the one hand, a redundancy of B cells that would not get sufficiently signaled by a comparatively small number of compatible T cells, and on the other hand, a waste of T cells in signaling a comparatively small number of B cells. For a schematic representation of the signalling between T cells and B clones see Figure 1.

Finally, B clones expand (contract) when they receive excitatory (inhibitory) signals by active T cells and compete for survival, so that each B clone follows a logistic dynamics

$$\frac{dB_{\mu}}{dt} = \frac{B_{\mu}}{cN^{1-\gamma}} \left(\lambda_{\mu} \sum_i \zeta_i^{\mu} \eta_i \sigma_i - \delta_{\mu} B_{\mu} - \frac{1}{n} \pi_{\mu}^{+} \Psi_{\mu} \right) \quad (14)$$

where the denominator in the prefactor represents the carrying capacity of the system for clone μ when all cognate T-helpers are activated and sending excitatory signal to clone μ and Ψ_{μ} represents the number of antigens of type μ . The prefactor

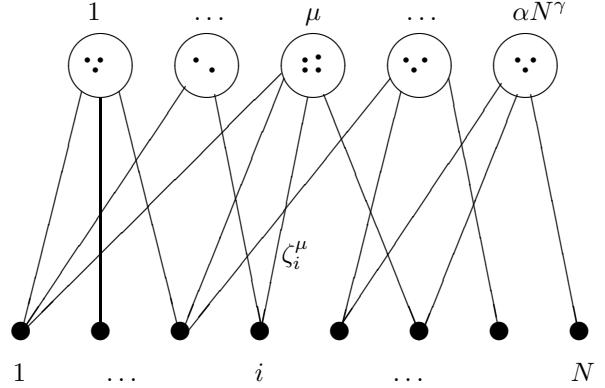


Figure 1: Schematic representation of the interactions between T cells and B clones. A link ζ_i^{μ} between T cell i and B clone μ means that T cell i can bind to B cells in clone μ . The number of T cells signaling a clone μ is of the same order as the number of B cells in clone μ , assumed $\mathcal{O}(N^{1-\gamma})$. In the figure, these numbers are chosen as $\mathcal{O}(1)$ and identical and are meant for illustration only.

n^{-1} of the third term accounts for the fact that upon binding an antigen, a B cell only engages one of its n receptors, so that the resulting APC is still a B cell, with one spare receptor less, which leads to a decrease of the effective number of B cells by a fraction $1/n$ only. In terms of population density, we have

$$\frac{db_{\mu}}{dt} = \lambda_{\mu} b_{\mu} \left(\frac{1}{cN^{1-\gamma}} \sum_i \zeta_i^{\mu} \eta_i \sigma_i - \frac{\delta_{\mu}}{\lambda_{\mu}} b_{\mu} - \frac{\pi_{\mu}^{+}}{\lambda_{\mu} n} \psi_{\mu} \right) \quad (15)$$

where the growth term is now proportional to the density of the net excitatory signal received by B clone μ from T cells, that we shall denote as

$$m_{\mu}(\boldsymbol{\sigma}) = \frac{1}{cN^{1-\gamma}} \sum_i \sigma_i \eta_i \zeta_i^{\mu} \quad (16)$$

with $\boldsymbol{\sigma} = (\sigma_1, \dots, \sigma_N)$ representing the microstate (active or inactive) of all T cells. Finally, bearing in mind that $n = \mathcal{O}(10^4)$, and neglecting $\mathcal{O}(n^{-1})$ in (15), we get

$$\frac{d}{dt} b_{\mu} = \lambda_{\mu} b_{\mu} \left(m(\boldsymbol{\sigma}) - \frac{\delta_{\mu}}{\lambda_{\mu}} b_{\mu} \right) \quad (17)$$

Denoting by $\mathcal{P}(z \leq x) = \int_{-\infty}^x dz p(z)$ the cumulative distribution function of the noise distribution $p(z)$, it follows from equation (12) that the likelihood to observe configuration σ_i at time $t + \Delta$, is, for any symmetric distribution $p(z) = p(-z)$,

$$p_{t+\Delta}(\sigma_i) = \mathcal{P} \left(z \leq (2\sigma_i - 1)\beta \sum_{\mu} \zeta_i^{\mu} p_{\mu}(t) \right)$$

where $\beta = 1/T$ is the inverse noise level. A natural choice for $p(z)$ would be a Gaussian distribution, that leads to $\mathcal{P}(z \leq x) = \frac{1}{2}(1 + \text{erf}(x/\sqrt{2}))$. An alternative choice is the so-called Glauber distribution (commonly made in statistical physics) leading to

$$\mathcal{P}(z \leq x) = \frac{1}{2} \left(1 + \tanh \frac{x}{2} \right),$$

qualitatively very similar to the cumulative distribution function for the Gaussian distribution and easier to work with analytically. For this choice, the probability that helper T cell i changes in a single time step its state σ_i at time t (to $1 - \sigma_i$ at time $t + \Delta$) is

$$W_t(\sigma_i) = \frac{1}{2} \left[1 + (1 - 2\sigma_i) \tanh \frac{\beta}{2} \sum_{\mu} \zeta_i^{\mu} p_{\mu}(t) \right]$$

where we used $1 - 2\sigma_i = \pm 1$ and $\tanh(\pm x) = \pm \tanh x$. Assuming that the update of T cells is sequential, i.e. at each time step one helper cell i , drawn at random, is updated with likelihood $W_t(\sigma_i)$, one obtains, for $\Delta = 1/N$ and N large, the following master equation for the probability density $p_t(\boldsymbol{\sigma})$ to observe microstate $\boldsymbol{\sigma}$ at time t ,

$$\frac{d}{dt} p_t(\boldsymbol{\sigma}) = \sum_i [p_t(F_i \boldsymbol{\sigma}) W_t(1 - \sigma_i) - p_t(\boldsymbol{\sigma}) W_t(\sigma_i)] \quad (18)$$

where F_i is a ‘‘cell-flip’’ operator that changes the configuration of T cell i from σ_i to $1 - \sigma_i$ and has no effect on any other cell $j \neq i$. From (18) one can derive equations of motion for the expectations $\langle \cdot \rangle = \sum \boldsymbol{\sigma} \cdot p_t(\boldsymbol{\sigma})$. Multiplying (18) by σ_j and summing over $\boldsymbol{\sigma}$, we obtain the following equation

$$\frac{d}{dt} \langle \sigma_j \rangle = \langle (1 - 2\sigma_j) W_t(\sigma_j) \rangle \quad (19)$$

intuitively meaning that the rate of change of the average activity of T cell j is given by its variation $1 - 2\sigma_j$ upon a single cell flip F_j , times the rate

$W_t(\sigma_j)$ at which the cell is flipped. Multiplying (19) times $\eta_j \zeta_j^{\mu}$ and summing over j , we obtain the following equation of motion for the average signal strength $m_{\mu}(t) = \langle m_{\mu}(\boldsymbol{\sigma}(t)) \rangle$ on clone μ :

$$\frac{dm_{\mu}}{dt} = \frac{N^{\gamma}}{2c} \langle \zeta^{\mu} \eta [1 + \tanh \frac{\beta}{2} \sum_{\nu} \zeta^{\nu} p_{\nu}] \rangle_{\eta, \zeta} - m_{\mu} \quad (20)$$

In the above $\langle \dots \rangle_{\eta, \zeta}$ denotes the average $\sum_{\eta, \zeta} \dots P(\eta, \zeta)$ over the distribution of regulatory patterns in the system (46).

Assuming that $P(\eta, \zeta) = P(\eta)P(\zeta)$ i.e. the ability of a helper cell i to bind to clone μ does not depend on whether i is a helper or regulator, we have

$$\frac{dm_{\mu}}{dt} = \frac{\epsilon N^{\gamma}}{2c} \langle \zeta^{\mu} [1 + \tanh \frac{\beta}{2} \sum_{\nu} \zeta^{\nu} p_{\nu}] \rangle_{\zeta} - m_{\mu}. \quad (21)$$

Finally, averaging over ζ^{μ} , using the independence of the ζ^{μ} 's and $\langle \zeta^{\mu} \rangle = c/N^{\gamma}$, we get

$$\frac{dm_{\mu}}{dt} = \frac{\epsilon}{2} \left[1 + \langle \tanh \frac{\beta}{2} (p_{\mu} + \sum_{\nu \neq \mu} \zeta^{\nu} p_{\nu}) \rangle_{\{\zeta^{\nu}\}} \right] - m_{\mu}, \quad (22)$$

where one has still to carry out the average over the $\{\zeta^{\nu}\}$ other than ζ^{μ} . At first glance, one may naively expect that equation (22) does not close, as m_{μ} depends on the whole set of $\{p_{\nu}\}$, and each p_{μ} depends, via (8), on b_{μ} and ψ_{μ} . The latter is determined from b_{μ} , however the former depends, via (17), on $m_{\mu}(\boldsymbol{\sigma})$, which is a priori different from the m_{μ} sitting in (22), defined as the average of $m_{\mu}(\boldsymbol{\sigma})$. However, one can show (see Appendix A) that for $\gamma < 1$, fluctuations of $m_{\mu}(\boldsymbol{\sigma})$ about its thermodynamic average m_{μ} vanish for large N . This allows us to replace $m_{\mu}(\boldsymbol{\sigma})$ in (17) with m_{μ} giving

$$\frac{db_{\mu}}{dt} = \lambda_{\mu} b_{\mu} \left(m_{\mu} - \frac{\delta_{\mu}}{\lambda_{\mu}} b_{\mu} \right) \quad (23)$$

This finally enable us to express the dynamical evolution of this immune system model in terms of a closed set of first order differential equations, namely (8), (9), (22) and (23). Equation (8) implies that the equilibrium density of antigen presenting cells is given, for all μ , by

$$p_{\mu} = a_{\mu} b_{\mu} \psi_{\mu} \quad (24)$$

where $a_{\mu} = \pi_{\mu}^{+} / \pi_{\mu}^{-}$ quantifies the affinity between

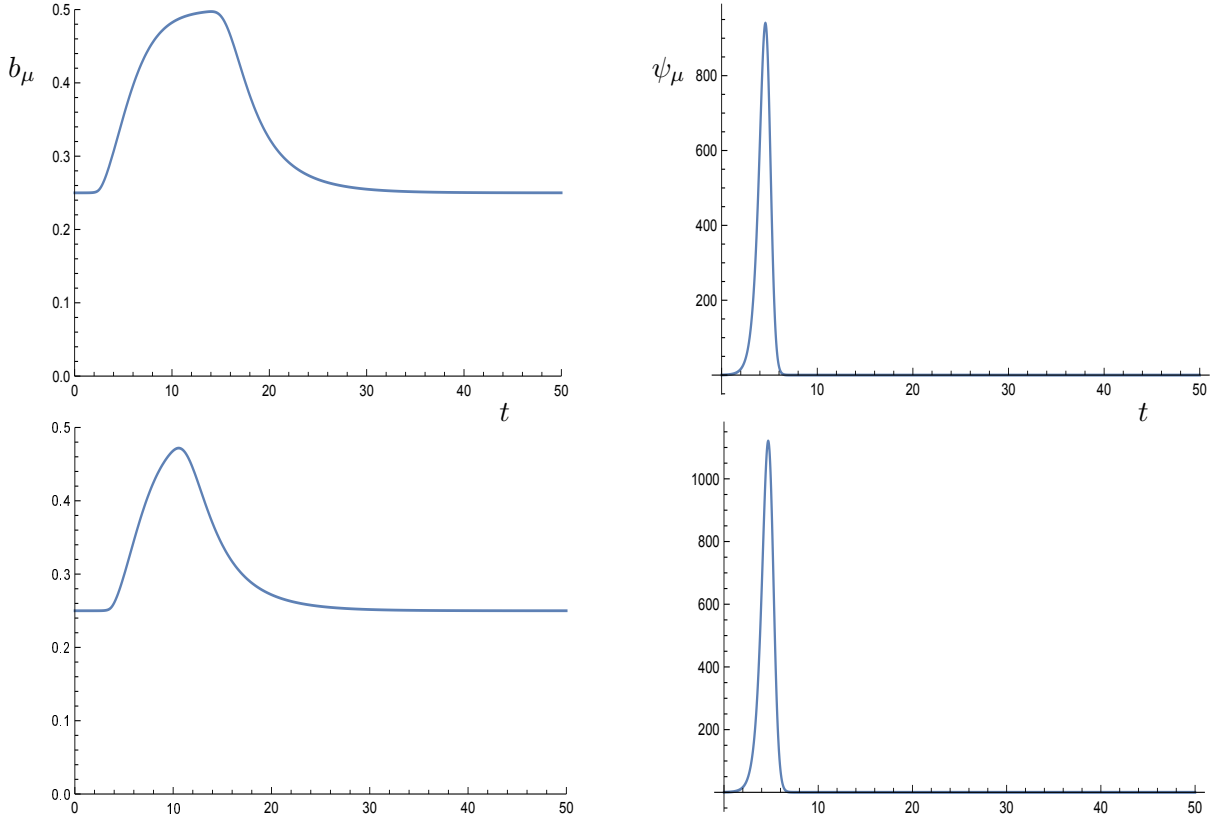


Figure 2: Time evolution of B clonal density b_μ (left) and antigen concentration ψ_μ (right) for $r_\mu = 2$, $\epsilon = 0.5$, $\lambda_\mu = \delta_\mu = \pi_\mu^- = 1$ and $\pi_\mu^+ = 10 \times [\tanh(10) + \tanh(t - 5)]$. Top panels: $\beta = 10$. Bottom panels: $\beta = 0.1$; Initial conditions were chosen as $\psi_\mu(0) = 0.3$, $b_\mu(0) = \kappa_\mu m_\mu(0)$, $m_\mu(0) = \epsilon/2$ and $p_\mu(0) = 0$. For higher noise levels $T = \beta^{-1}$, the system mounts a weaker immune response, resulting in lower B clonal densities and higher antigen concentrations, however the antigen is still removed within the same timescale.

B clone μ and antigen μ .⁴ If the system is initially in equilibrium in the absence of antigen, one has $p_\mu = 0 \forall \mu$, and from (22) we get $m_\mu = \epsilon/2 \forall \mu$. Hence, equation (23) yields $b_\mu = \kappa_\mu \epsilon/2$, with $\kappa_\mu = \lambda_\mu/\delta_\mu$, for $\epsilon > 0$, and $b_\mu = 0$ for $\epsilon < 0$.

3.1 Response to a single antigen

In this section, we study the activation of the immune system when a single antigen type μ is present, i.e. $\psi_\mu \neq 0$ and $\psi_\nu = 0 \forall \nu \neq \mu$.

Assuming that, when antigen μ is introduced in the host at time $t = 0$, the latter is resting at its equilibrium state in the absence of antigen, we have for all $t > 0$ and all $\nu \neq \mu$

$$(\psi_\nu, p_\nu, m_\nu, b_\nu) = \left(0, 0, \frac{\epsilon}{2}, \max\left\{0, \frac{\kappa_\nu \epsilon}{2}\right\}\right), \quad (25)$$

⁴The affinity can be experimentally measured as the ratio between the equilibrium concentration of APC and the product of the equilibrium concentrations of antigen and specific B cells.

as for $\psi_\nu = 0$, $p_\nu = 0$ is a fixed point of the dynamics (8), and from (22) we get

$$\begin{aligned} \frac{dm_\nu}{dt} &= \frac{\epsilon}{2} \left[1 + \langle \tanh \frac{\beta}{2} \zeta^\mu p_\mu \rangle_{\xi^\mu}\right] - m_\nu \\ &= \frac{\epsilon}{2} - m_\nu + \mathcal{O}(N^{-\gamma}), \end{aligned} \quad (26)$$

of which $m_\nu = \epsilon/2$ is a fixed point, for large N . In contrast, equation (22) gives for clone μ , that is compatible with the antigen introduced in the host,

$$\frac{dm_\mu}{dt} = \frac{\epsilon}{2} \left[1 + \tanh \frac{\beta}{2} p_\mu\right] - m_\mu \quad (27)$$

whose stationary solution is, inserting (24),

$$m_\mu = \frac{\epsilon}{2} \left[1 + \tanh \frac{\beta}{2} a_\mu b_\mu \psi_\mu\right] \quad (28)$$

where b_μ and ψ_μ are the steady state solutions of (23) and (9), respectively. Equation (28) shows that at stationarity $m_\mu > 0$ for any $\epsilon > 0$, so the stable steady state of (23) is $b_\mu = \kappa_\mu m_\mu$.

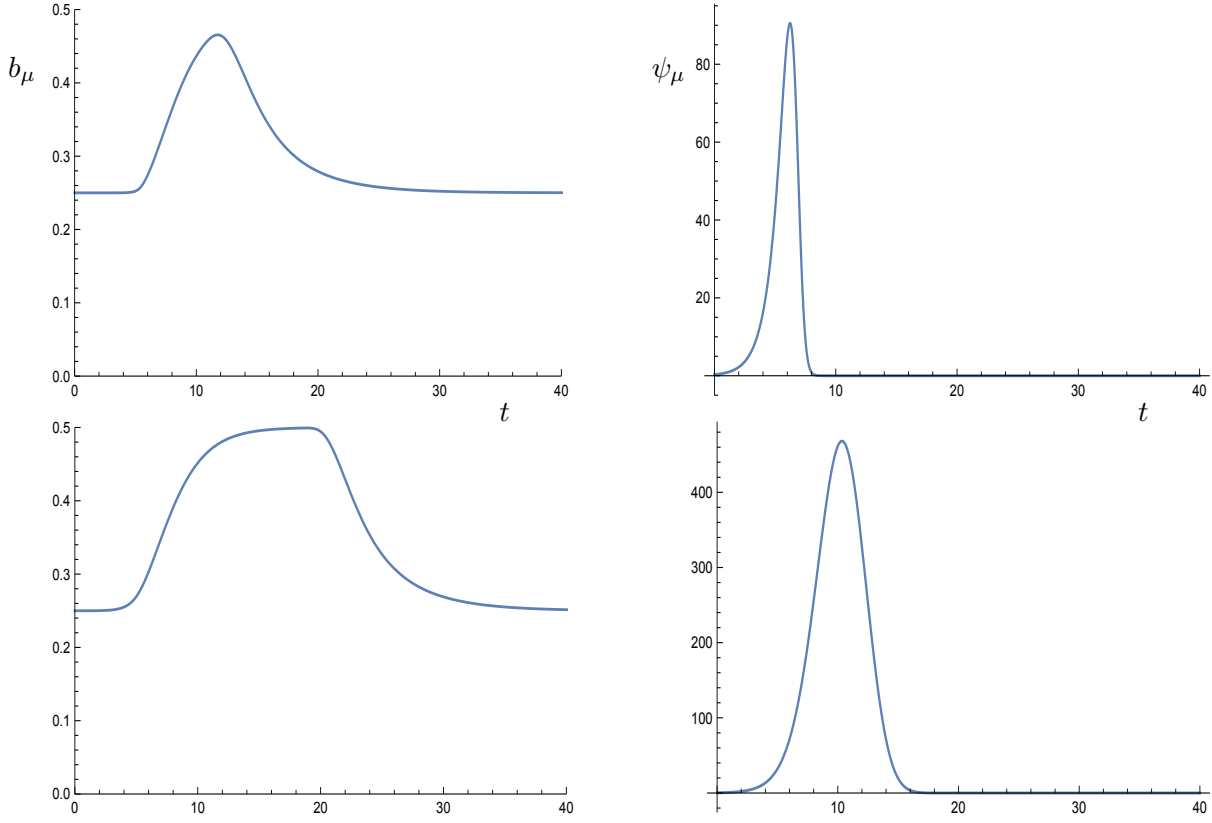


Figure 3: Time evolution of B clonal density b_μ (left) and antigen concentration ψ_μ (right) for $r_\mu = 1$, $\epsilon = 0.5$, $\lambda_\mu = \delta_\mu = \pi_\mu^- = 1$ and $\beta = 1$. Top panels: $\pi_\mu^+ = 10 \times [\tanh(10) + \tanh(t - 7)]$. Bottom panels: $\pi_\mu^+ = 10 \times [\tanh(2.01) + \tanh[(t - 20)/10]]$. Initial conditions were chosen as in Figure 2. The time-dependence of the affinity maturation π_μ^+ affects both the intensity of viral concentration and the timescale on which viral removal is accomplished.

This yields, for the stationary value of m_μ , the solution of the self-consistency equation

$$m_\mu = \frac{\epsilon}{2} \left[1 + \tanh \frac{\beta \kappa_\mu}{2} a_\mu \psi_\mu m_\mu \right] \quad (29)$$

where ψ_μ is the steady state solution of

$$\frac{d}{dt} \psi_\mu = \psi_\mu (r_\mu - \kappa_\mu \pi_\mu^+ m_\mu). \quad (30)$$

One can see that $(\psi_\mu, m_\mu) = (0, \epsilon/2)$ is the only stable fixed point of this dynamical system for $\pi_\mu^+ > 2r_\mu/\epsilon\kappa_\mu$, meaning that for $\epsilon > 0$, antigen removal is accomplished when the affinity of the antigen-specific BCR is large enough compared to the antigen replication rate. Conversely, for $\pi_\mu^+ < 2r_\mu/\epsilon\kappa_\mu$, the fixed point $(0, \epsilon/2)$ becomes unstable and different types of dynamics may arise, depending on the range of the kinetic parameters. Since $0 \leq \tanh(\beta a_\mu b_\mu \psi_\mu / 2) \leq 1$, one has, from (28), $\epsilon/2 \leq m_\mu \leq \epsilon$, hence the largest value attainable by m_μ is ϵ . Then (30) implies that

for $\pi_\mu^+ < r_\mu/\epsilon\kappa_\mu$, the viral concentration will grow indefinitely, whereas for $r_\mu/\epsilon\kappa_\mu < \pi_\mu^+ < 2r_\mu/\epsilon\kappa_\mu$, the system will settle, after a transient, onto a limit cycle, where $m_\mu(t)$ oscillates between two values m_- , m_+ , with $\epsilon/2 \leq m_- < m_+ \leq \epsilon$, such that $r_\mu - \kappa_\mu \pi_\mu^+ m_- > 0$ and $r_\mu - \kappa_\mu \pi_\mu^+ m_+ < 0$. This leads to a periodic motion of viral concentration, meaning that the antigen will permance indefinitely in the host, but its growth is limited by the action of the immune system.

As B cells undergo clonal expansion, they increase their affinity with the antigen, via affinity maturation, so π_μ^+ is an increasing function of time. For the model in study here, this implies that, as long as $\epsilon > 0$, the system will eventually reach the affinity value $\pi_\mu^+ = 2r_\mu/\epsilon\kappa_\mu$ where the fixed point $(\psi_\mu, m_\mu) = (0, \epsilon/2)$ becomes stable and the system will manage to remove the antigen completely.

In contrast, for $\epsilon \leq 0$, we get from (28) $m_\mu \leq 0$, so the stable fixed point of (23) is $b_\mu = 0$, which

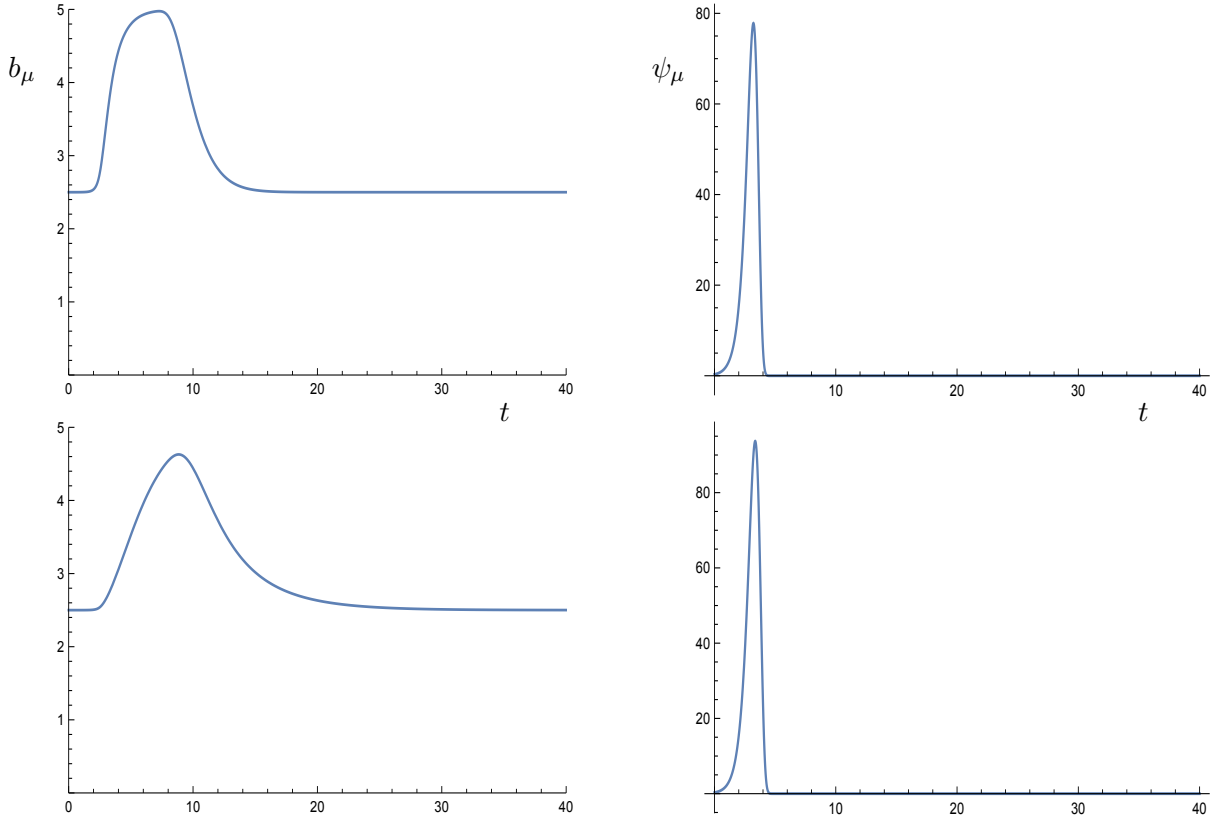


Figure 4: Time evolution of B clonal density b_μ (left) and antigen concentration ψ_μ (right) for $\beta = 1$, $\pi_\mu^+ = 10 \times [\tanh(10) + \tanh(t - 5)]$, $\pi_\mu^- = 1$, $r = 2$ and $\epsilon = 0.5$. Top panels: $\lambda_\mu = 10$ and $\delta_\mu = 1$. Bottom panels: $\lambda_\mu = 1$, $\delta_\mu = 0.1$. Initial conditions were chosen as in Figure 2

inserted into (28) and (9), leads to $m_\mu = -|\epsilon|/2$ and to an antigen indefinitely replicating in the host through $d\psi_\mu/dt = r_\mu\psi_\mu$, no matter how fast or large π_μ^+ is growing.

We show the results of numerical solution of (23), (9), (27) and (8) in Figures 2, 3, 4 and 5, where b_μ and ψ_μ are plotted as a function of time for different choices of the inverse noise level β (Fig. 2), time-dependence of π_μ^+ (Fig. 3), different values of the kinetic parameters λ_μ , δ_μ (Fig. 4), and for different values of π_μ^- and antigen replication rate r_μ (Fig. 5). On the assumption that the affinity is an increasing function of time that saturates at large time, $\pi_\mu^+(t)$ was chosen as the following sigmoid function:

$$\pi_\mu^+(t) = \pi_M[\pi_0 + \tanh(\gamma(t - t^*))] \quad (31)$$

where γ , t^* , π_M and π_0 are parameters that control, respectively, how fast, early and large the affinity grows and its initial value. Since the affinity is experimentally found to increase by four or five orders of magnitude over a period of a week, we chose $t^* \leq 7$ and π_0 such

that the ratio $\pi_\mu^+(\infty)/\pi_\mu^+(0) = (\pi_0 + 1)/(\pi_0 - \tanh \gamma t^*)$ between the final and the initial value of π_μ^+ is $\mathcal{O}(10^4 - 10^5)$. However, the actual time-dependence of π_μ^+ has no qualitative impact on the immune response, as long as it is an increasing function, whose limit is $\pi_\mu^+(\infty) > 2r_\mu/\epsilon\kappa_\mu$. Plots show an immune response that follows perfectly the behaviour of the antigen, i.e. it expands B clones while the antigen concentration is increasing and contracts them when the antigen concentration is decreasing, so that both the B clone concentration and the antigen concentration are unimodal functions of time. The stochastic noise T has the effect of mildly reducing the height of the peak in B clones concentration, thus increasing the peak in viral concentration, however the system will be able to remove the antigen even at high noise levels (see Fig. 2). The time-dependence of π_μ^+ , affects both the location and the height of the peaks, consistently with the intuition that the faster the affinity grows, the earlier and the smaller the peak in viral concentration. Fig. 3 shows that the affinity that starts increas-

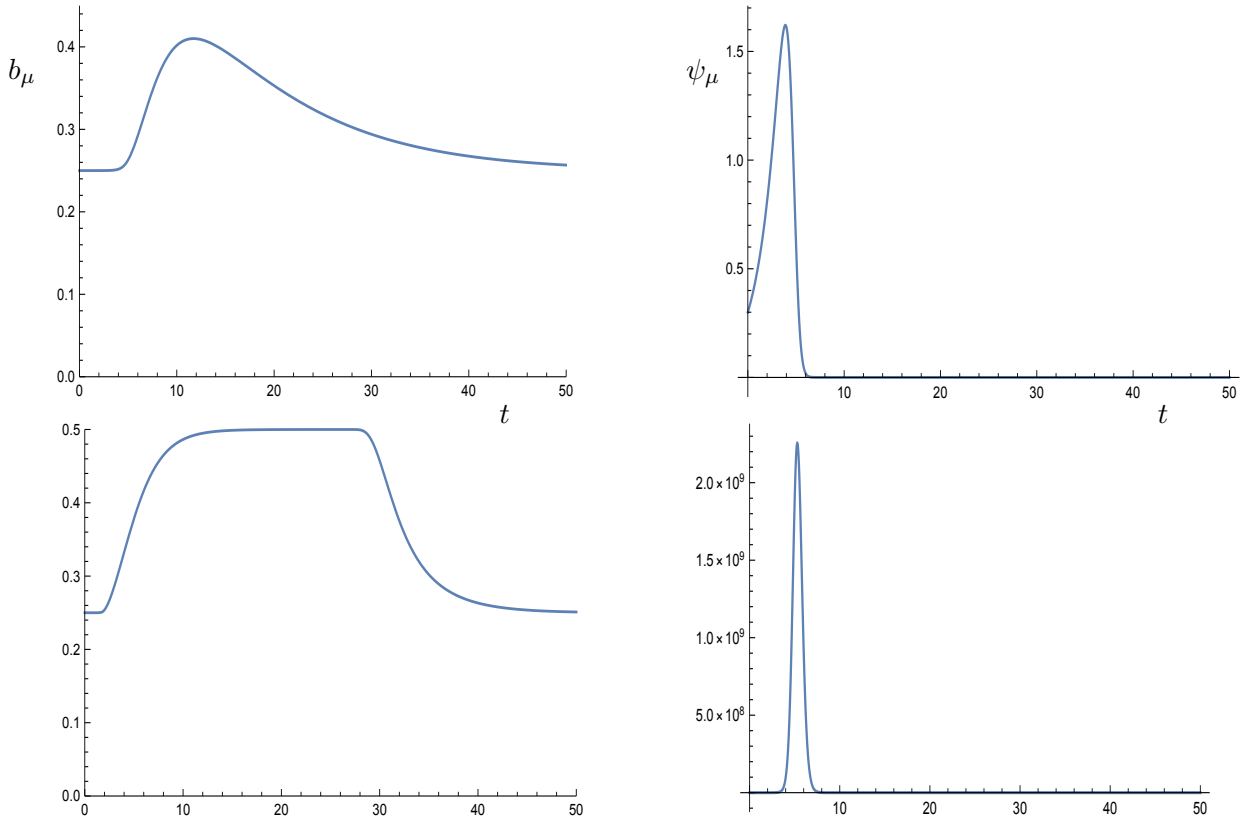


Figure 5: Time evolution of B clonal density b_μ (left) and antigen concentration ψ_μ (right) for $\beta = 1$, $\pi_\mu^+ = 10 \times [\tanh(10) + \tanh(t - 5)]$, $\lambda_\mu = \delta_\mu = 1$ and $\epsilon = 0.5$. Top panels: $r = 0.5$ and $\pi_\mu^- = 0.1$. Bottom panels: $r = 5$, $\pi_\mu^- = 1$. Initial conditions were chosen as in Figure 2.

ing at day $t^* = 7$ with rate $\gamma = 1$ outperforms the affinity that starts increasing at day $t^* = 20$ with a slower rate $\gamma = 1/10$. The kinetic parameters λ_μ and δ_μ have a mild effect on the shape of the B clonal concentration (see Fig. 4), while Fig. 5 (top panel) shows that π_μ^- affects more noticeably the decay of B cells after the infection peak, potentially sustaining long-term memory. Finally, Fig. 5 (bottom panel) shows that although faster-replicating antigens will attain much higher concentrations, they are still removed, for positive values of ϵ , within similar timescales, by triggering a stronger immune response.

In contrast, Fig. 6 shows that as soon as ϵ is lowered below zero, the system becomes unresponsive and is not able to fight a single antigen, even if replicating slowly. Our results suggest that for Th/Treg ratios $R > 1$ the host manages to remove completely the antigen and the time it takes depends on how large and fast the affinity π_μ^+ between BCR and antigen grows. Conversely, for $R < 1$ the immune system is impaired and infections will permene indefinitely in the host.

More in general, this model captures the effectiveness of the adaptive immune system in dealing with very diverse scenarios and predicts that the most important single parameter in determining whether the system is in a healthy or in an immuno-suppressed phase is ϵ , directly related to the Th/Treg ratio R via (11) and in line with recent experiments [36, 37, 41]. Finally, we note that although unstable, $b_\mu = 0$ is always a fixed point of (23), even for $\epsilon > 0$. This suggests that a fast mutating pathogen (like e.g. cancerous cells or HIV) that manages to release new (i.e. mutated) types of antigens in the host, before being removed from the system, may succeed in escaping the immune system, by eventually mutating to a form μ^* for which there is no answering B cell, i.e. $b_{\mu^*} = 0$. Given that B cells responding to self-antigens are suppressed via negative selection processes occurring in the bone marrow, one way for a non-self antigen to escape the immune system is to mutate to a form close to self-antigens, as it occurs in HIV. Another way is to disrupt the mechanism by which non-self antigens are flagged up as such, by

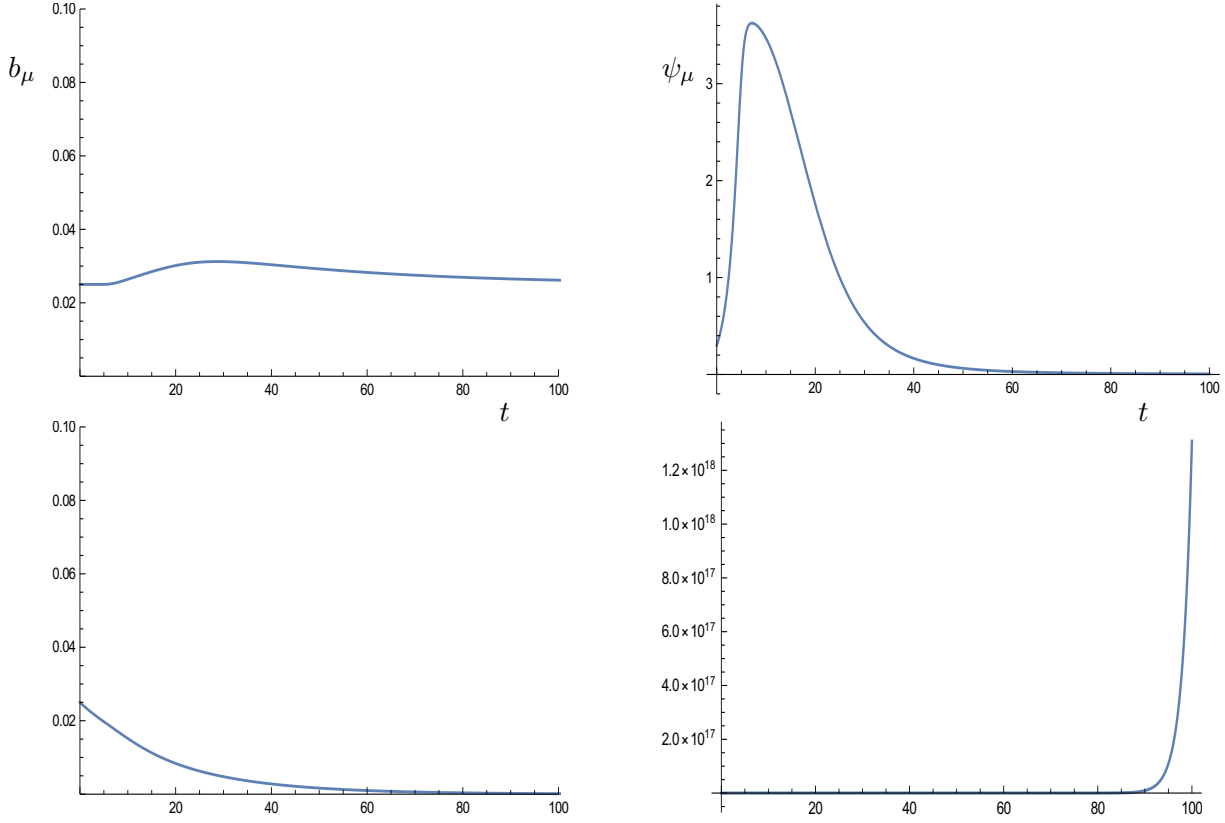


Figure 6: Time evolution of B clonal density b_μ (left) and antigen concentration ψ_μ for $\beta = 1$, $\pi_\mu^+ = 10 \times [\tanh(10) + \tanh(t - 5)]$, $\pi_\mu^- = 1$, $\lambda_\mu = 5$, $\delta_\mu = 1$, $r_\mu = 0.5$. In the top panels $\epsilon = 0.01$, while in bottom panels $\epsilon = -0.01$. Initial conditions were chosen as $\psi(0) = 0.3$ and $b_\mu(0) = \kappa_\mu |\epsilon|/2$. The plot shows that as soon as $\epsilon < 0$ the system cannot remove the antigen.

e.g. altering the functionality of MHC molecules, a pattern that has been observed both in cancer and HIV progression [52, 53]. This second route would make $\zeta_i^\mu = 0 \forall i$, so that $m_\mu = 0$ and the density of responding B cells becomes $b_\mu = 0$.

3.2 The role played by the mechanism that activates Tregs

The activation of Treg cells is still quite debated. Above we assumed that Treg cells get activated in the same way as Th cells, i.e. by binding to an APC. However, there is no general consensus about the need of antigen mediation [54].

This prompts us to consider an alternative version of the model used above, where the mechanism that activates Th cells remains the same, while activation of Treg cells is fully stochastic

$$\sigma_i(t + \Delta) = \theta \left(\frac{1 + \eta_i}{2} \sum_\mu \zeta_i^\mu p_\mu(t) - Tz(t) \right) \quad (32)$$

i.e. for $\eta_i = -1$ the activation of i is determined

by a random variable, while for $\eta_i = 1$ we have the same equation as before. Repeating the steps that led to (22), we get

$$\frac{dm_\mu}{dt} = \frac{N^\gamma}{2c} \langle \zeta^\mu \eta [1 + \tanh \frac{\beta}{2} \frac{1 + \eta}{2} \sum_\nu \zeta^\nu p_\nu] \rangle_{\eta, \zeta} - m_\mu \quad (33)$$

that simplifies, in the single antigen case, to

$$\frac{dm_\mu}{dt} = \frac{1}{2} \left[\epsilon + \frac{1 + \epsilon}{2} \tanh \frac{\beta}{2} p_\mu \right] - m_\mu \quad (34)$$

For $\epsilon > 0$, the stationary solution of (34) is $m_\mu > 0$, hence the stationary solution of (23) is $b_\mu = \kappa_\mu m_\mu$ where m_μ solves the self-consistency equation

$$m_\mu = \frac{1}{2} \left[\epsilon + \frac{1 + \epsilon}{2} \tanh \frac{\beta}{2} a_\mu \psi_\mu \kappa_\mu m_\mu \right] \quad (35)$$

The solution is easily found in terms of the shifted variables $M_\mu = m_\mu - \epsilon/2$ by intersecting the curves

$$M_\mu = \frac{1 + \epsilon}{4} \tanh x \quad (36)$$

$$M_\mu = \frac{2x}{\beta \kappa_\mu a_\mu \psi_\mu} - \frac{\epsilon}{2} \quad (37)$$

that we plot in Figure 7 (top panels) for different values of the parameters. Note that the intercept of (37) with the M_μ -axis is smaller in modulus than the minimum value attainable by M_μ in (36) i.e. $|\epsilon/2| < |(1 + \epsilon)/4|$ for $0 \leq \epsilon < 1$, in contrast with the previous case, where these values coincided (as the prefactor of $\tanh x$ in (29) was $\epsilon/2$).

For $\epsilon > 0$ we have a stable positive solution $0 < M_\mu < (1 + \epsilon)/4$ for any finite $\psi_\mu > 0$ (see Fig. 7, top left panel), meaning that the system is able to mount a response, potentially stronger than before, as the maximum value $(1 + \epsilon)/4$ attainable by M_μ is larger than the earlier maximum $\epsilon/2$. However, in contrast with the previous scenario, two additional, negative, solutions will appear (see Fig. 7, top right panel) for $\psi_\mu \geq \psi^*$, value at which the straight line (37) becomes tangent to the curve (36) at the value of x where the two curves intersect. (This situation could not arise in the previous scenario, as, there, the straight line would intersect the M_μ axis at the minimum value attainable by the sigmoid curve). One can show that the inner of these solutions is unstable, while the outer two are stable. For any initial value of M_μ to the right of the unstable solution, (provided the system is in the regime of parameters where this exists), the system will evolve to the stable positive solution and the antigen will be removed in a similar fashion as before and even slightly earlier, given the larger value attainable by M_μ . This will include in particular initialization of the system at its resting value in the absence of antigen, i.e. $M_\mu = 0$.

However, if the system is initialized with a sufficiently negative value of M_μ , it may end up, for large enough values of the antigen concentration, in a state of undesired immunosuppression $M_\mu < -\epsilon/2$, i.e. $m_\mu < 0$, in which case b_μ evolves to zero and the system becomes unresponsive. We note that immunosuppressed initial conditions might be reached also by means of statistical fluctuations of $M_\mu(\sigma)$ with respect to its average value M_μ . Although we expect these fluctuations to be negligible for large N and $\gamma < 1$, they will get relevant in the regime $\gamma = 1$ (see Appendix A).

For $\epsilon < 0$ we have a stable negative solution for any finite $\psi_\mu > 0$ with two additional positive solutions, one stable and one unstable, appearing for $\psi_\mu \geq \psi^*$, and the system will always evolve

towards the negative stable solution (corresponding to immunosuppression), unless it is initialised at large enough values of M_μ and antigen concentration is high enough.

In conclusion, the Treg activation mechanism considered here, leads, for any realistic initial condition, to a scenario qualitatively very similar to the previous one, with the antigen effectively removed for $\epsilon > 0$ and indefinitely growing for $\epsilon < 0$, but we have also noted the possibility of undesired behavior emerging for extreme initial conditions, or attainable by means of statistical fluctuations, that we expect to become important in the regime $\gamma = 1$.

The scenario remains very similar if we assume that activation of Treg cells, instead of following the same mechanism as Th cells, or being performed stochastically, follows a mechanism opposite to Th cells, whereby Treg cells get inhibited by the presence of APCs. One may speculate that this might actually be a desired feature for the immune system if it has to suppress immune responses which are not solicited by antigens and inhibit repression mechanisms in the presence of antigens. Such a mechanism is modelled by

$$\sigma_i(t + \Delta) = \theta \left(\eta_i \sum_{\mu} \zeta_i^{\mu} p_{\mu}(t) - Tz(t) \right) \quad (38)$$

which leads to

$$\frac{dm_{\mu}}{dt} = \frac{N^{\gamma}}{2c} \langle \zeta^{\mu} \eta \left[1 + \tanh \frac{\beta}{2} \eta \sum_{\nu} \zeta^{\nu} p_{\nu} \right] \rangle_{\eta, \zeta} - m_{\mu} \quad (39)$$

This simplifies, for the single antigen case, to

$$\frac{dm_{\mu}}{dt} = \frac{1}{2} \left[\epsilon + \tanh \frac{\beta}{2} p_{\mu} \right] - m_{\mu} \quad (40)$$

Since $\tanh x \geq 0 \forall x \geq 0$, for $\epsilon > 0$, at stationarity $m_{\mu} > 0$ and $p_{\mu} = \kappa_{\mu} a_{\mu} \psi_{\mu} m_{\mu}$. Hence, the stationary value of $m_{\mu} = M_{\mu} + \epsilon/2$ is found by intersecting the two curves

$$M_{\mu} = \frac{1}{2} \tanh x \quad (41)$$

$$M_{\mu} = \frac{2x}{\beta \kappa_{\mu} a_{\mu} \psi_{\mu}} - \frac{\epsilon}{2} \quad (42)$$

Their plot in Figure 7 (bottom panels) shows that we have a stable positive solution $0 \leq M_{\mu} \leq 1/2$ for any finite $\psi_{\mu} > 0$, meaning that the immune

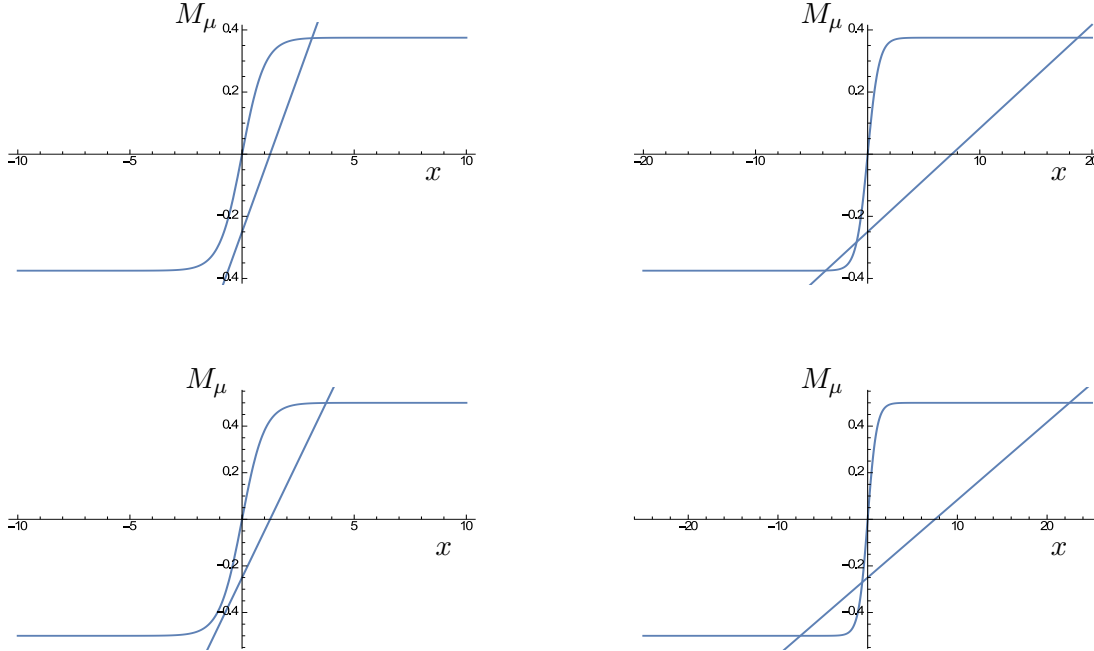


Figure 7: Top panels: curves (36) and (37) for $\epsilon = 0.5$, $\beta = 10$, $a_\mu = 10$, $\kappa_\mu = 1$ and $\psi = 0.1$ (left) $\psi = 0.6$ (right). Bottom panels: curves (41) and (42) shown for the same parameters. In bottom panels, the maximum value attainable by M_μ is larger and the transition from one to three solutions occurs earlier, i.e. at a lower antigen concentration.

system is capable of a response even stronger than before (given $1/2 \geq (1 + \epsilon)/4$ for $0 \leq \epsilon \leq 1$). Similarly to the previous scenario, two additional, negative, solutions will appear for $\psi_\mu \geq \tilde{\psi}$, value at which the straight line (42) becomes tangent to the curve (41) at the value of x where the two curves intersect (note that $\tilde{\psi} < \psi^*$). Hence, this scenario behaves qualitatively very similarly to the previous one, with the antigen effectively removed for $\epsilon > 0$ and indefinitely growing for $\epsilon < 0$ for any realistic initial condition. With respect to the scenario analysed previously, the present scenario leads, on the one hand, to a slightly stronger immune response, but on the other hand, to the possibility of undesired behavior arising from a slightly larger basin of (still extreme) initial conditions.

In conclusion, the exact mechanism that activates Treg cells does not seem to play a crucial role, as much as their relative number with respect to Th cells, to the extent that even a fully stochastic activation of Treg cells would result in a sensible immune response, for any realistic initial condition. This may explain the existence of different types of suppressor T cells, some antigen-specific and some nonspecific [51]. Nonetheless, our anal-

ysis shows that the safest activation mechanism, i.e. ensuring a sensible response for *any* initial condition, is the one mediated by the antigen.

4 Conclusions

In this work, we introduced a statistical mechanical model for the adaptive immune system, which comprises B cells, Th cells, Treg cells and antigens. We investigated the scenario where Treg cells can directly suppress B cells and considered different mechanisms for Treg activation (elicited/inhibited by the antigen or fully stochastic). When the ratio between T helper and T regulatory cells is above one, the model produces an immune response which is a unimodal function of time, in qualitative agreement with experimental observations, accomplishing, in particular, a complete removal of the antigen, for any chosen value of the control parameters (replication rates, cell death rates and noise level) and any chosen increasing function of time for the affinity between B cells and antigens. In addition, the model is very resilient to changes in the particular mechanism that activates Treg cells, to the extent that even a fully

stochastic activation would lead to a sensible immune response, as long as the ratio between Th and Treg cells is above one. Importantly, the model shows an abrupt change in its behaviour when the ratio between Th and Treg cells is lowered below one, showing in particular a phase transition from a functional to an impaired phase.

To the best of our knowledge, this is the first mathematical model with a predictive power on the effect of the Th/Treg imbalance on the immune system dynamics and may offer a useful theoretical framework to complement and compare recent experimental studies aimed at assessing the validity of the Th/Treg ratio as a biological marker of immunosuppression. Our results are consistent, at stationarity, with the equilibrium statistical mechanical analysis carried out in [20], where the B cells density was shown to be a decreasing function of the Treg cells density, in equilibrium.

Possible pathways for future work include a detailed modelling of the affinity maturation of B cells in the germinal centre, the clonal expansion of active T cells, and stochasticity effects in the dynamics of non-T cells. In addition, one may consider the presence of dendritic cells and other immune cells that can act as antigen presenting cells, threshold effects in the activation of T cells, and different regimes of dilution in the interactions between B and T cells. Further studies may focus on the effect of fast mutating antigens like cancerous cells and retrovirus, that manage to mutate before being removed from the system, and the mechanism by which HIV infection and cancer progression alter the Th/Treg ratio. Finally, we have restricted our analysis to a single epitope antigen, however, antigens have normally several epitopes which may be recognized by different B clones, so that cross-reactivity effects may be included in future extensions of this model.

We hope that even at this level of simplification, the model can stimulate debate on several unclear aspects of Tregs functioning and their role in immunosuppression.

5 Acknowledgements

It is my pleasure to thank Alexander Mozeika for many interesting discussions.

References

- [1] RJ De Boer, IG Kevrekidis, AS Perelson (1990), *Chem. Eng. Sci.* **45**: 2375–2382.
- [2] MA Nowak, RM May (2000), *Virus Dynamics: Mathematical Principles of Immunology and Virology*, Oxford University Press (New York)
- [3] K León, A Lage, J Carneiro (2003), *J. Theor. Biol.* **225**(1): 107–126.
- [4] NJ Burroughs, BMPM de Oliveira, AA Pinto (2006), *J. Theor. Biol.* **241**(1): 13–141.
- [5] D Fouchet, R Regoes (2008) *PLoS ONE* **3**(5): e2306.
- [6] HK Alexander and LM Wahl (2011) *Bull. Math. Biol.* **73**(1): 33–71.
- [7] G Bogle, PR Dunbar (2009), *Immunol. Cell Biol.* **88**(2):172179.
- [8] F Chiacchio, M Pennisi, G Russo, *et al.* (2014), *BioMed Research International* **2014**: 907171.
- [9] A Scherer, M Salathe, S Bonhoeffer (2006), *PLoS Comput. Biol.* **2**(8): e109.
- [10] A Casal, C Sumen, TE Reddy, *et al.* (2005), *J. Theor. Biol.* **236**(4): 376–391.
- [11] MT Figge (2009), *PLoS ONE* **4**(5): e5685.
- [12] A Barra, E Agliari (2010) *Physica A* **389**(24): 5903–5911.
- [13] ER Stirka, G Lythea, HA van den Bergb, C Molina-Pars (2010), *J. Theor. Biol.* **265**(3): 396–410.
- [14] J Reynolds, IF Amado, AA Freitas, *at al.* (2014), *J. Theor. Biol.* **347**:160-175.
- [15] Parisi G (1990) *Proc. Natl. Acad. Sci. USA* **87**(1): 429 –433.
- [16] A Barra, E Agliari (2010) *J Stat Mech: Th. Exp.* P07004.
- [17] E Agliari, A Annibale, A Barra, *et al.* (2013), *J. Phys. A: Math. Theor:* **46**:415003.

- [18] S Bartolucci, A Annibale, (2015) *J. Stat. Mech: Th. Exp.* **2015**(8):P08017.
- [19] S Bartolucci, A Mozeika, A Annibale (2016) *J. Stat. Mech: Th. Exp.* **2016**(8):083402.
- [20] A Mozeika, ACC Coolen (2016) pre-print: arXiv:1603.01328
- [21] RJ De Boer, AS Perelson (1990), *J. Theor. Biol.* **149**(3): 381424.
- [22] A Madi, DY Kenett, S Bransburg-Zabary, *et al. PLoS ONE* **6**(3):e17445.
- [23] T Mora, AM Walczak, W Bialek, CG Callan (2010) *Proc. Natl. Acad. Sci.* **107**(12): 5405–5410.
- [24] L Asti, G Uguzzoni, P Marcatili, A Pagnani (2016) *PLoS Comput. Biol.* **12**(4): e1004870.
- [25] J Greene, MR Birtwistle, L Ignatowicz, GA Rempala (2013) *J. Theor. Biol.* **326**:1–10.
- [26] L Boelen, PK O’Neill, R Boyton, *et al.* (2014) *IMMUNOLOGY* **143**:185-186.
- [27] L Boelen, PK O’Neill, KJ Quigley *et al.*, 2016, *Plos Comput. Biol.* **12**(3):e1004796.
- [28] M Castro, G Lythe, C Molina-Paris, RM Ribeiro (2016) *Interface Focus* **6**:20150093.
- [29] PS Kim, D Levy and PP Lee (2009) *Methods Enzymol.* **467**:79–109
- [30] J Mestas, CCW Hughes (2004) *J. Immunol.* **172**(5):2731-2738
- [31] S Sakaguchi, K Wing, M Miyara (2007) *Eur. J. Immunol.* **37**:S116–23.
- [32] N Ohkura, Y Kitagawa, S Sakaguchi (2013) *Immunity.* **38**(3):414-23
- [33] I Wollenberg, A Agua-Doce, A Hernandez, *et al.* (2011), *J Immunol.* **187**(9):4553-60.
- [34] IK Gratz, MD Rosenblum, AK Abbas AK (2013), *Ann. N. Y. Acad. Sci.* **1283**:8–12.
- [35] Hyoun-Il Kim, MD Haeryoung, MD Hyoun Won Cho, *et al.* (2011), *Journal of Surgical Oncology*, **104**:728–733.
- [36] F Brivio, L Fumagalli, D Parolini, *et al.* (2008), *In vivo* **22**(5):647-650.
- [37] JM Valverde-Villegas, MC Cotta Matte, RM de Medeiros, JA Bogo Chies (2015), *Journal of Immunology Research*, 647916.
- [38] B Miles, SM Miller, JM Folkvord *et al.* (2015), *Nature Communications* **6**:8608
- [39] D Li, J Chen, M Jia, *et al.* (2011), *Clin. Exp. Immunol.* **165**(3): 363-371
- [40] S Serrano-Villar, S Moreno, M Fuentes-Ferrer, *et al.* (2014), *HIV Med.* **15**(1):40-49
- [41] ZX Yu, MS Ji, J Yan, *et al.* (2015), *Critical Care* **19**(1):82.
- [42] M Caridade, L Graca, RM Ribeiro (2013) *Front Immunol.* **4**: 378.
- [43] J Carneiro, T Paixoa, D Milutinovich, *et al.* (2005) *Journal of Computational and Applied Mathematics* **184**(1): 77–100.
- [44] NS. De Silva, U Klein (2015), *Nature reviews Immunology* **15**: 137–148.
- [45] A Corthay (2009), *Scand. J. Immunol.* **70**(4): 326–336.
- [46] BM Hall, GT Tran, ND Verma, *et al.* (2013), *Front. Immunol.* **4**:208.
- [47] P Wang, S G Zheng (2013) *Int. J. Clin. Exp. Pathol.* **6**(12):2668–2674.
- [48] J Gotot, C Gottschalk, S Leopold, *et al.* (2012) *PNAS* **109**(26):10468–10473
- [49] HW Lim, P Hillsamer, AH Banham, CH Kim (2005) *J. Immunol.* **175**(7):4180–4183.
- [50] N Iikuni, EV Loureno, BH Hahn, A La Cava, (2009) *J. Immunol.* **183**(3):1518–1522.
- [51] L Majlessi, R Lo-Man, C Leclerc (2008), *Microbes and Infection* **10**:1030–1035.
- [52] S Yoshihama, J Roszik, I Downs, *et al.* (2016), *PNAS* **113**(21):5999–6004.
- [53] W Kamp, MB Berk, CJ Visser, HS Nottet (2000), *Eur. J. Clin. Invest.*, **30**(8):740–6.
- [54] S Sakaguchi, N Sakaguchi, M Asano, *et al.* (1995), *J. Immunol.* **155**(3):1151–1164.

A The Kramers-Moyal expansion of the master equation

In this section, we use the master equation (18) for the evolution of the probability density $p_t(\boldsymbol{\sigma})$, to derive dynamical equations for the macroscopic parameters $\mathbf{m}(\boldsymbol{\sigma}) = (m_1(\boldsymbol{\sigma}), \dots, m_P(\boldsymbol{\sigma}))$.

As a first step, we derive an equation for the probability density $\mathcal{P}(\mathbf{m}) = \sum_{\boldsymbol{\sigma}} P(\boldsymbol{\sigma}) \delta(\mathbf{m} - \mathbf{m}(\boldsymbol{\sigma}))$ that the macroscopic parameters $\mathbf{m}(\boldsymbol{\sigma})$ take values \mathbf{m}

$$\begin{aligned} \partial_t \mathcal{P}(\mathbf{m}) &= \\ &= \sum_{\boldsymbol{\sigma}} \delta(\mathbf{m} - \mathbf{m}(\boldsymbol{\sigma})) \sum_i [p_t(F_i \boldsymbol{\sigma}) W_t(1 - \sigma_i) - p_t(\boldsymbol{\sigma}) W_t(\sigma_i)] \\ &= \sum_{\boldsymbol{\sigma}} \sum_i p_t(\boldsymbol{\sigma}) W_t(\sigma_i) [\delta(\mathbf{m} - \mathbf{m}(F_i \boldsymbol{\sigma})) - \delta(\mathbf{m} - \mathbf{m}(\boldsymbol{\sigma}))] \end{aligned} \quad (43)$$

Next we work out the change $\Delta_{i\mu}$ occurring in the parameter $m_\mu(\boldsymbol{\sigma})$ when spin i is flipped

$$\Delta_{i\mu} = m_\mu(F_i \boldsymbol{\sigma}) - m_\mu(\boldsymbol{\sigma}) = \frac{1}{cN^{1-\gamma}} (1 - 2\sigma_i) \eta_i \zeta_i^\mu$$

Expanding (43) in powers of $\Delta_{i\mu}$ we obtain

$$\begin{aligned} \partial_t \mathcal{P}(\mathbf{m}) &= \\ &= \sum_{\boldsymbol{\sigma}} \sum_i p_t(\boldsymbol{\sigma}) W_t(\sigma_i) \left[- \sum_{\mu} \Delta_{i\mu} \frac{\partial}{\partial m_\mu} \delta(\mathbf{m} - \mathbf{m}(\boldsymbol{\sigma})) \right. \\ &\quad \left. + \frac{1}{2} \sum_{\mu\nu} \Delta_{i\mu} \Delta_{i\nu} \frac{\partial^2}{\partial m_\mu \partial m_\nu} \delta(\mathbf{m} - \mathbf{m}(\boldsymbol{\sigma})) + \dots \right] \end{aligned} \quad (44)$$

Next, we work out

$$\begin{aligned} & \sum_i W_t(\sigma_i) \Delta_{i\mu} = \\ &= \frac{1}{2cN^{1-\gamma}} \sum_i \left[1 - 2\sigma_i + \tanh \frac{\beta}{2} \zeta_i^\nu p_\nu \right] \eta_i \zeta_i^\mu \\ &= -m_\mu(\boldsymbol{\sigma}) + \frac{N^\gamma}{2c} \langle \eta \xi^\mu [1 + \tanh \frac{\beta}{2} \sum_\nu \xi^\nu p_\nu] \rangle \end{aligned} \quad (45)$$

where in the last step the average over all T helper cells for one specific realization of regulatory effects $(\eta_1, \dots, \eta_N, \zeta_1, \dots, \zeta_N)$, has been replaced by the average over the distribution of regulatory effects for one single helper cell

$$P(\eta, \zeta) = \lim_{N \rightarrow \infty} \frac{1}{N} \sum_{j=1}^N \delta_{\eta, \eta_j} \delta_{\zeta, \zeta_j} \quad (46)$$

where $\delta_{x,y} = 1$ for $x = y$ and $\delta_{x,y} = 0$ otherwise, and $\zeta_j = (\zeta_j^1, \dots, \zeta_j^P)$ encodes the regulatory interactions between B cells and T cell j . If the number N of vectors (η_i, ζ_i) is much larger than the number 2^{P+1} of possible vectors (η, ζ) , this replacement is justified by appealing to the law of large numbers. However, for larger P , this statement is non-trivial and relies on the assumption of what is called, in statistical physics jargon, “self-averageness”, according to which a physical observable in a macroscopic system does not depend on the particular realization of the microscopic variables $\{\eta_i, \zeta_i^\mu\}$ but only on the distribution $P(\eta, \zeta)$ they are sampled from. Noting that (45) depends on $\boldsymbol{\sigma}$ only through $m_\mu(\boldsymbol{\sigma})$, we can write

$$\sum_i W_t(\sigma_i) \Delta_{i\mu} = f_\mu(m_\mu(\boldsymbol{\sigma}), \mathbf{p}) \quad (47)$$

Inserting (47) into (43), using the constraint $m_\mu(\boldsymbol{\sigma}) = m_\mu$ to remove the $\boldsymbol{\sigma}$ -dependence of f_μ and carrying out the summation over $\boldsymbol{\sigma}$, we obtain

$$\partial_t \mathcal{P}(\mathbf{m}) = - \sum_{\mu} \frac{\partial}{\partial m_\mu} [f_\mu(m_\mu, \mathbf{p}) \mathcal{P}(\mathbf{m})] + \dots (48)$$

One can show that higher order terms, arising from the second term in the square brackets of (43), are at most $\mathcal{O}(N^{\gamma-1})$, hence for large N and $\gamma < 1$ they vanish. In this limit, (48) becomes a Liouville equation, that corresponds to the below deterministic evolution for the parameters \mathbf{m}

$$\partial_t m_\mu = \frac{N^\gamma}{2c} \langle \eta \xi^\mu [1 + \tanh \frac{\beta}{2} \sum_\nu \xi^\nu p_\nu] \rangle - m_\mu \quad (49)$$

For large but finite values of N , fluctuations of the stochastic parameters $m_\mu(\boldsymbol{\sigma})$ about the deterministic values $m_\mu = \langle m_\mu(\boldsymbol{\sigma}) \rangle$ will be $\mathcal{O}(N^{(\gamma-1)/2})$.